55th ARFTG Conf. Dig., pp. 116-121, Boston, June 16, 2000. Presented by D. C. DeGroot.

ANALYSIS OF INTERCONNECTION NETWORKS AND MISMATCH IN THE NOSE-TO-NOSE CALIBRATION

Donald C. DeGroot[a] and Paul D. Hale[b]
National Institute of Standards and Technology
[a]*Radio-Frequency Technology Division,* [b]*Optoelectronics Division*
325 Broadway, Boulder, CO 80303-3328 USA
Phone: 303-497-7212; Fax: 303-497-3970; E-mail degroot@nist.gov

Marc Vanden Bossche, Frans Verbeyst, and Jan Verspecht
Agilent Technologies, Inc., NMDG, VUB/ELEC, Pleinlaan 2, B-1050 Brussels, Belgium

ABSTRACT

We analyze the input networks of the samplers used in the nose-to-nose calibration method. Our model demonstrates that the required input network conditions are satisfied in this method and shows the interconnection errors are limited to measurement uncertainties of input reflection coefficients and adapter *S*-parameters utilized during the calibration procedure. Further, the input network model fully includes the effects of mismatch reflections, and we use the model to reconcile nose-to-nose waveform correction methods with traditional signal power measurement techniques.

I. INTRODUCTION

The nose-to-nose calibration [1] provides an estimate for the response of a broadband oscilloscope and the means to deconvolve that response from a measured signal. The calibration provides one of the only means of obtaining total phase relations of the frequency components in a broadband signal (up to 50 GHz). Certain conditions that are not usually required in traditional calibrations must be met for the nose-to-nose method to work. While many of these conditions have been studied in previous works [1-3], the first section of this paper examines the requirement of identical forward and reverse transfer functions for the internal interconnection networks. The second section uses this understanding to develop an equivalence between oscilloscope-based measurements of signal power and traditional power-meter techniques. This equivalence may be used for verifying the magnitude response of the nose-to-nose calibration.

II. NOSE-TO-NOSE INPUT NETWORK

When performing a nose-to-nose calibration, one oscilloscope sampler is configured to generate a kick-out pulse, and a second is configured to receive, sample, and digitize the pulse. A single nose-to-nose measurement M gives the convolution of two sampler responses. In the frequency domain:

$$M_{ij}(\omega) = K_j(\omega)H_i(\omega), \tag{1}$$

where $K_j(\omega)$ is the frequency-domain representation of the kick-out pulse from sampler j, and $H_i(\omega)$ is the forward transfer function of sampler i. If the kick-out of a given sampler is proportional to its forward response ($K_i \propto H_i$), a series of three measurements ($M_{ij} = K_j H_i$) on three sampler heads provides an estimate of H. For example:

$$H_A = \sqrt{\frac{M_{AB} M_{AC}}{M_{BC}}}. \tag{2}$$

In previous analyses [1-3], the input network and sampler electronic responses were combined in deriving overall expressions for H and K. Here, we are interested in isolating the input network response. To do so, we define H' and K' to be the transfer function and kick-out response of the sampling electronics when an impedance $Z_c/2$ is connected to the sampling node. Figure 1a shows K' being generated at that sampling node, though we would actually measure K at the front panel connector. Likewise H' is the transfer function from that sampling node to the measured data M, though we would actually determine an overall H that would include the interconnection networks.

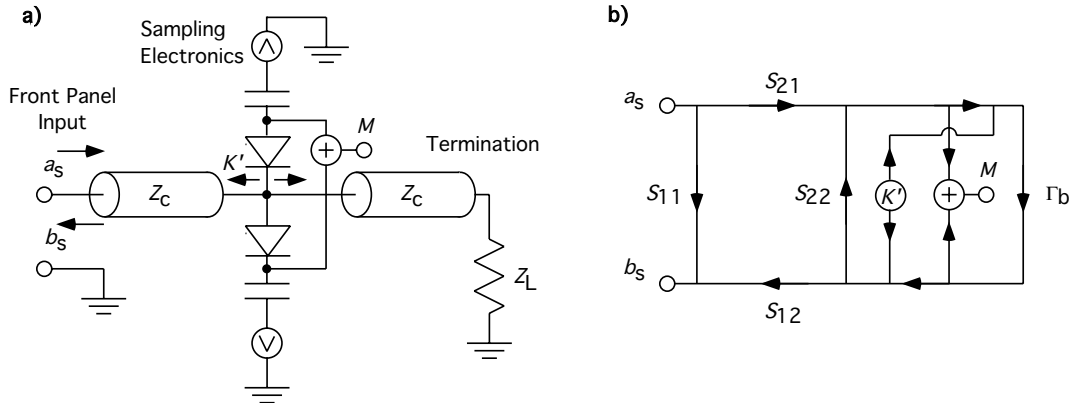

Fig. 1 (a) Schematic and (b) flow-diagram representations of sampler head electronics and interconnection networks.

In order to separate the sampling electronics from the interconnection networks, we must first ensure one condition and realize another. First, the input network must have a longer round-trip delay time than the sampling aperture time ($\tau_d > \tau_a$). This is necessary since an unwanted sampler pulse is generated for any nonzero input, and reflections of this pulse could add with the input if they arrived at the sampling node before the sampling aperture closed. Second, we must realize, as Refs. [1-3] show, that both H' and K' are dependent on the impedance presented by the interconnection network at the sampling node during the time the diodes are conducting[1]. In other words, H' and K' are functions of the network impedance Z_c during the duration of the short kick-out pulse ($\approx \tau_a$). These conditions allow us to separate the input network response

[1] Equations 4.2-42 and 4.2-43 of Ref. [3] approximate K and H with functions that depend on S_{22} of the interconnection network. Since S_{22} depends on the impedance of the network, defining K' and H' as functions of Z_c is consistent with Ref. [3].

from the sampler electronics response and examine the necessary conditions of the input network.

Figure 1a models the sampler electronics and shows how kick-out pulses and input signals are modified by the interconnection networks. We use this schematic representation to develop a flow-diagram model of the circuit signals. As shown in Fig. 1b, the back-end network can be replaced with a single reflection coefficient. When measuring an input signal, the sampler measures the sum of the incident wave plus multiple reflections of the back-end and front-end networks. When generating kick-out pulses, the sampler output b_s is a combination of K' and multiple internal reflections of K'. Assuming linearity, we reduce the flow-diagram model of Fig. 1b to the equivalent two-port network illustrated in Fig. 2. The elements of the equivalent two-port network are determined by solving Fig. 1b:

$$\mathbf{S}' = \begin{bmatrix} \dfrac{S_{11} + \Gamma_b S_{21} S_{12} - \Gamma_b S_{11} S_{22}}{1 - \Gamma_b S_{22}} & \dfrac{(1+\Gamma_b) S_{12}}{1 - \Gamma_b S_{22}} \\ \dfrac{(1+\Gamma_b) S_{21}}{1 - \Gamma_b S_{22}} & \dfrac{S_{22} + \Gamma_b + 2\Gamma_b S_{22}}{1 - \Gamma_b S_{22}} \end{bmatrix}, \tag{3}$$

where S_{ij} are the scattering parameters of the front-end network in Fig. 1, and Γ_b represents the reflections of the termination and back-end network.

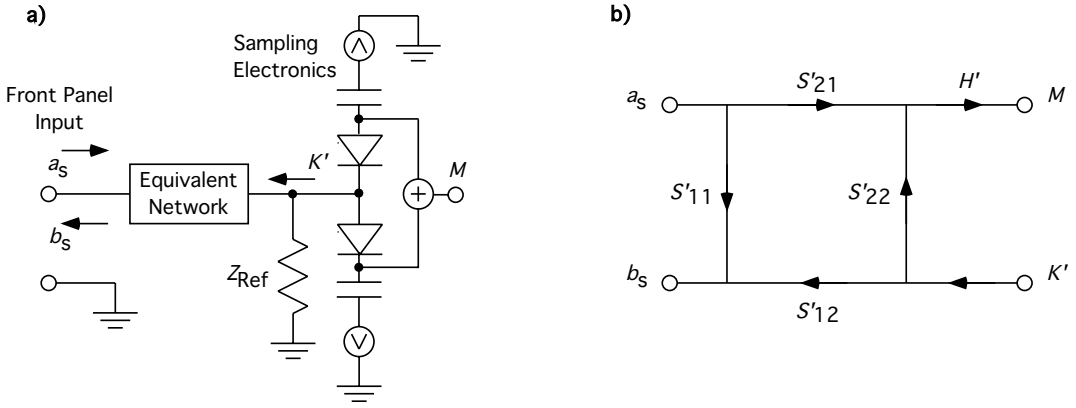

Fig 2. Equivalent (a) schematic and (b) flow diagram representations of sampler interconnection network.

If we could access a measurement port at the sampling-node location, we could determine the values of $\mathbf{S}'$ directly. Since this is not possible, we need to assess the interconnection network effects by combining the terms of $\mathbf{S}'$ with the kick-out K' and transfer function H' of the sampling electronics, in the same manner as a nose-to-nose measurement:

$$M_{ij} = K'_j S'^{j}_{12} \bullet H'_i S'^{i}_{21}. \tag{4}$$

With Eqn. (4), we solve Eqn. (2) for the overall forward transfer function from a set of three measurements:

$$H_A = \sqrt{\frac{M_{AB}M_{AC}}{M_{BC}}} = H'_A S'^{A}_{21} \sqrt{\frac{K_B S'^{B}_{12}}{H_B S'^{B}_{21}}} = cH'_A S'^{A}_{21} \sqrt{\frac{S'^{B}_{12}}{S'^{B}_{21}}}, \tag{5}$$

where c is the real constant relating K_B to H_B; that is, $K_B = cH_B$.

If $K_B \propto H_B$, as required, then the reciprocity condition $S'^{\,B}_{12} = S'^{\,B}_{21}$ provides an estimate for H_A from a set of three nose-to-nose measurements. Though $\mathbf{S}'$ is not symmetric, it is reciprocal as long as the front-end network is reciprocal, and this condition is met.

Whether or not reciprocity is a necessary condition depends on the use of the nose-to-nose calibration. The nose-to-nose calibration does not require $K_i = H_i$, it requires only that the forward transfer function be simply proportional to the kick-out response. In practice, the frequency dependence of the response is the desired result, since the real scaling factor c can be determined from supporting measurements. If one only needs to determine H_i values to within an undetermined constant, then $S'_{12} \propto S'_{21}$ becomes a sufficient condition.

III. INPUT NETWORK ANALYSIS FOR SIGNAL POWER MEASUREMENTS

The ability of a nose-to-nose calibration to successfully estimate a given H_i can be verified in part by comparing signal power measurements of a frequency-swept oscillator with nose-to-nose corrected measurements of the same signal source. In making these comparisons [1,3,4], we encountered different nomenclature and methods used in power meter measurements [5,6]. We show how these two approaches are reconciled.

To measure the signal power of a source, a power sensor can be connected directly to the source output (Fig. 3a). Since the power sensor responds to net delivered power, two correction factors are required to correlate the measurement P_m with incident signal power $|a_m|^2$:

$$P_m = \eta\left(|a_m|^2 - |b_m|^2\right) = \eta|a_m|^2\left(1 - |\Gamma_m|^2\right), \tag{6}$$

where $1-|\Gamma_m|^2$ is known as the mismatch loss and accounts for the power reflected by the sensor, and η is known as the sensor efficiency and accounts for ohmic and radiation losses in the sensor interconnection and housing. Both of these factors are used to correct measured incident power in commercial power meters.

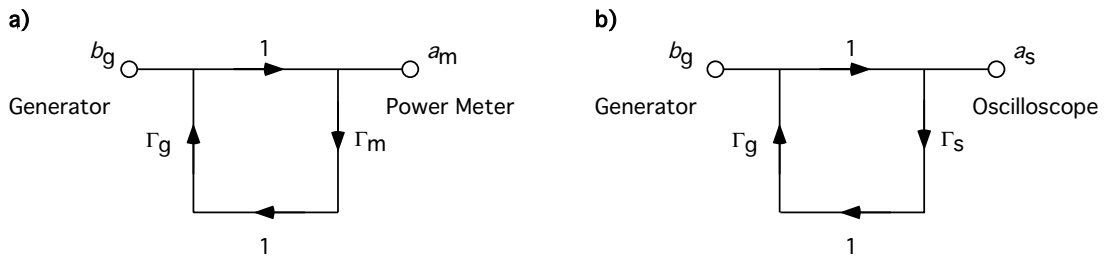

Fig. 3 Flow diagram notation for a source connected to (a) a power meter and (b) an oscilloscope.

With vector measurements of the generator and meter reflection coefficients Γ_g and Γ_m, respectively, the power of the incident signal a_m can be related to the power of the source b_g:

$$|a_m|^2 = \frac{|b_g|^2}{|1-\Gamma_g\Gamma_m|^2}, \tag{7}$$

where $|1-\Gamma_g\Gamma_m|^2$ is known as the mismatch uncertainty. If only the magnitudes $|\Gamma_g|$ and $|\Gamma_m|$ are known, P_g can only be bounded, which is the original reason for the terminology, mismatch uncertainty.

Combining Eqns. (6) and (7) gives the source power in terms of the measured value and the calibration terms:

$$|b_g|^2 = \frac{P_m|1-\Gamma_g\Gamma_m|^2}{\eta\left(1-|\Gamma_m|^2\right)}. \tag{8}$$

When using an oscilloscope to measure the power output of a signal generator, the nose-to-nose correction determines how the amplitude and phase of the displayed voltage wave are modified relative to the input voltage wave when both are defined for a given reference impedance (such as $Z_{ref} = 50\ \Omega$). The total forward transfer function $H(\omega)$ includes both ohmic and mismatch effects for the specific interconnection network **S′** and sampler circuit *H′*. To measure signal power with an oscilloscope, the source is connected directly to the scope input (Fig. 3b). The measured data $M(\omega)$ are corrected with $H(\omega)$ to give a_s. With known Γ_g and Γ_s, a_s can be corrected to give b_g. Squaring the magnitude of the source voltage wave gives us a second determination of source power:

$$|b_g|^2 = \frac{|M|^2|1-\Gamma_g\Gamma_s|^2}{|H|^2}. \tag{9}$$

Since b_g is the invariant that relates our power meter measurement with our oscilloscope measurement, we can equate Eqns. (8) and (9) to derive an expression for $|H|$ in terms of a measured power and the reflection coefficients:

$$|H| = \frac{|M||1-\Gamma_g\Gamma_s|}{|1-\Gamma_g\Gamma_m|}\sqrt{\frac{\eta\left(1-|\Gamma_m|^2\right)}{P_m}}. \tag{10}$$

This expression provides the means to calibrate the oscilloscope's magnitude response against a reference power meter. It is important to note that Eqn. (10) differs from that used when calibrating an unknown power sensor against a reference sensor [7], because the scope responds to signal voltage instead of net delivered power. It would be erroneous to further correct a calibrated oscilloscope measurement with an oscilloscope mismatch loss term (that is, $1 - |\Gamma_s|^2$).

Equation (10) also provides the means to verify part of the nose-to-nose estimate for a sampler's forward transfer function. It provides a model that predicts measurement uncertainty for the power meter/nose-to-nose comparison described by Hale *et al.* [4] using adapter and sampler reflection coefficient measurements; it provides the means to determine whether $|H_i|$ estimated by the nose-to-nose method agrees with that determined from power measurements of a frequency-swept source.

IV. CONCLUSIONS

We have analyzed the interconnection networks of the samplers used in the nose-to-nose calibration. Assuming linearity and the conditions necessary to isolate sampling electronics from the passive interconnection network, we developed an equivalent two-port network and solved for the terms in the matrix. If the interconnection between the front panel connector and the sampling node is reciprocal, our analysis demonstrates that the nose-to-nose calibration will account for the passive internal networks appropriately. Therefore, interconnection errors are limited to those made when correcting for sampler mismatch and the adapter used to connect two sampler inputs together.

With an understanding of the equivalent two-port description of the oscilloscope sampler, we also developed a method by which the magnitude response of the scope can be calibrated against a reference power meter. This method may also be used to verify the success of the nose-to-nose calibration. With the equations we developed, our analysis can be further extended to bound the measurement uncertainty for the purposes of such comparisons.

ACKNOWLEDGMENTS

We thank Dr. Kate Remley for her helpful comments and assistance in this work.

REFERENCES

[1] J. Verspecht and K. Rush, "Individual characterization of broadband sampling oscilloscopes with a nose-to-nose calibration procedure," IEEE Transactions on Instrumentation and Measurement, vol. 43, no. 2, pp. 347-354, Apr., 1994.

[2] J. Verspecht, "Broadband sampling oscilloscope characterization with the "nose-to-nose": calibration procedure: A theoretical and practical analysis," IEEE Transactions on Instrumentation and Measurement, vol. 44, no. 6, pp. 991-997, Dec., 1995.

[3] J. Verspecht, "Calibration of a measurement system for high frequency nonlinear devices," Vrije Universiteit Brussel, Ph.D., 1995.

[4] P. D. Hale, T. S. Clement, K. J. Coakley, C. M. Wang, D. C. DeGroot, and A. P. Verdoni, "Estimating the magnitude and phase response of a 50 GHz sampling oscilloscope using the "nose-to-nose" method," *55th ARFTG Conf. Dig.*, June, 2000.

[5] G. F. Engen, Microwave Circuit Theory and Foundations of Microwave Metrology. London: Peter Peregrinus, Ltd., 1992.

[6] Hewlett-Packard Company, "Fundamentals of RF and Microwave Power Measurements", HP Application Note 64-1.

[7] J. R. Juroshek, "A direct calibration method for measuring equivalent source mismatch," *Microwave J.*, pp. 106-118, Oct., 1997.